Structure of supersonic jets with vortex generators at the nozzle exit

Valery I. Zapryagaev, Ivan N. Kavun and Nickolay P. Kiselev
Khristianovich Institute of Theoretical and Applied Mechanics, Siberian Branch, Russian Academy of Sciences, Novosibirsk, 630090, Russia, E-mail: zapr@itam.nsc.ru

Abstract
The spatial structure of the flow in a supersonic underexpanded jet exhausting from a convergent nozzle with vortex generators (chevrons) at the exit is experimentally studied. Disturbances of two types are observed during interaction of a single chevron and the main jet. The stronger disturbance is caused by the presence of the wake component and by generation of two streamwise vortices. The weaker disturbance is manifested in the form of perturbations of the Mach wave type propagating in the supersonic part of the shear layer of the main jet. Interaction of the set of chevrons with the jet flow leads to transformation of the stationary jet structure and to formation of mushroom-shaped large-scale vortex structures. The experimental and numerical data are demonstrated to be in reasonable agreement.

1. INTRODUCTION

Studying the mixing processes at supersonic flow velocities is important for development of effective and high-technology devices and vehicles. Such engineering devices include supersonic air-breathing engines (scramjets), ejectors with a high degree of flow compression, ejector-type thrust amplifiers, and devices for application of metallic coatings onto the surface. Intensification of mixing in the shear layer offers effective methods of jet noise reduction, which is another important task.

The difficulty of the problem considered is reduction of the mixing intensity with increasing flow velocity [1]. At high supersonic velocities, the spreading rate of the shear layer, i.e., an increase in the shear layer thickness in the dependence on the streamwise distance, decreases by a factor of 4-5, as compared to situations with low subsonic velocities of the flow [2]. This significant decrease in the mixing intensity is caused by stabilization of the shear layer at supersonic velocities.

An analysis of physical mechanisms of turbulent mixing in the shear layer indicates that one of the governing mechanisms of entrainment of external fluid into the jet flow is based on streamwise vortices [3]. Such vortex structures exist in the developed turbulent shear layer; their intensity and sizes are determined by the boundary conditions and flow parameters.

The possibility of generating streamwise vortices with the use of vortex generators, aimed at mixing intensification in the shear layer, has been studied for more than 20 years. Various methods are used to form streamwise vortex structures: lobed mixers, tabs, chevrons, and also injection of microjets into the main flow.

Zapryagaev and Solotchin [4] performed experiments in a nozzle without artificial disturbances and found that there are azimuthal inhomogeneities of the distributions of gas-dynamic quantities (pressure and density) in the shear layer of a supersonic jet. It was shown that these azimuthal inhomogeneities are caused by the presence of streamwise vortex structures of the Taylor-Goertler type [5]. One of the governing factors of the emergence of vortex structures in supersonic underexpanded jets is the curvature of streamlines [6]. The use of various vortex-forming elements at the nozzle exit leads to significant reconstruction of the jet flow and to formation of large-scale streamwise vortices in both supersonic and subsonic flows [7-9]. Artificial streamwise vortices intensify the process of gas mixing and reduce the level of noise generated by the jet [9, 10].

A tab is a projection (flap) located on the surface wetted by a gas or a liquid and acting on the flow by means of changing the flow structure [9]. A chevron is a vortex-forming element (vortex generator) shaped as a triangle (or a trapezoid) whose inner surface is a continuation of the inner surface of the nozzle exit [11]. These definitions are applicable to the vortex generator at the nozzle exit with exhaustion of a supersonic jet, because the character of flow interaction with the vortex generator depends on the exhaustion regime (pressure ratio at the nozzle exit).

The use of chevrons and tabs in nozzles of turbofan engines allows the jet noise to be substantially reduced. Optimal configurations of nozzles with chevrons and tabs were found, which made it possible to reduce the noise level by 2.7 dB with a minor loss in throat (approximately 0.06%) [11].

In addition to experimental research, numerical and theoretical methods of studying turbulent jet noise are also developed. Shur et al. [12] used large eddy simulation to study the mechanisms of noise generation and propagation in high-velocity and supersonic jets at high Reynolds numbers and also the formation of acoustic waves in complex jets exhausting from bypass nozzles and from nozzles with the central body. As a result, integral characteristics of the flow (thrust and mass flow) were obtained, and the influence of vortex generators on the jet noise was studied.

Despite numerous publications on mixing intensification in supersonic jets with the use of vortex generators for generating large-scale streamwise vortices, the structure of the modified jet flow has not been adequately examined. The objective of the present activities was an experimental and numerical study of the gas-dynamic flow structure at the initial section of a supersonic underexpanded jet exhausting from a nozzle with vortex-forming elements in the form of chevrons at the nozzle exit.

2. EXPERIMENTAL EQUIPMENT

The initial section of a supersonic nonisobaric jet with artificially generated vortex structures was experimentally studied in a jet module of a T-326 blowdown wind tunnel based at the Khristianovich Institute of Theoretical and Applied Mechanics of the Siberian Branch of the Russian Academy of Sciences. A photograph and a sketch of the jet module are shown in Figure 1. An axisymmetric jet exhausted into a 1.3×0.55×0.93 m test section 3. The pressure sensors were moved by an automated radial-azimuthal traversing gear 6 attached to the outer surface of the nozzle. The accuracy of its motion was 0.01 mm over the radius, 0.1 mm over the streamwise coordinate, and 0.2° over the azimuthal angle. The error of pressure measurement in the jet was 0.1%.

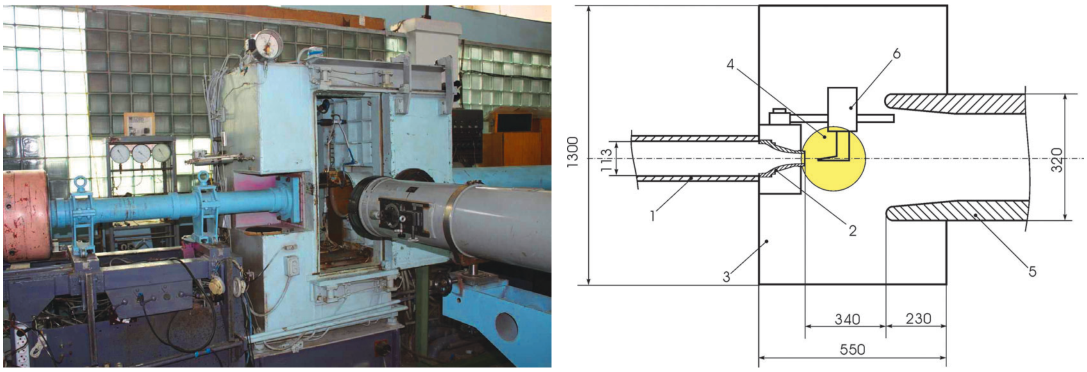

Figure 1. Photograph and sketch of the jet module of the T-326 hypersonic blowdown wind tunnel: 1 - settling chamber of the jet module; 2 - replaceable nozzles; 3 - test section; 4 - window; 5 - supersonic diffuser; 6 - radial-azimuthal traversing gear.

The experiments were performed in a convergent axisymmetric nozzle with the geometric Mach number in the exit section equal to $M_a = 1.0$ and with a polished inner surface (Figure 2.). The nozzle contour was calculated by the Vitoshinskii formula and ensured a smooth transition from the input to the output nozzle diameters [13]. The input diameter of the subsonic section was 88 mm, the nozzle exit diameter was 30 mm, and the nozzle length was 157 mm.

Special measures to improve the quality of the fabricated nozzle were taken to minimize uncontrolled disturbances in the shear layer of the jet, which are formed by microscopic roughness elements on the inner surface of the nozzle. Deviations of the inner surface of the nozzles from a circumference (nonroundness) were measured at a distance of 3 mm from the nozzle exit section by a 73PC roundness instrument produced by Taylor Rank. The measured nonroundness of the nozzles was $\varepsilon = 2.65\ \mu$m, which corresponds to $e/R_a = 0.02\%$. The surface roughness was measured during streamwise motion of the measurement tip in the vicinity of the nozzle exit section by a 120L profilometer produced by Form Talysurf. The mean surface roughness in the nozzles used, which was determined as the mean height of roughness elements on the profile, was $k \approx 0.25\ \mu$m. The boundary-layer thickness at the nozzle exit was $\delta \approx 1$ mm.

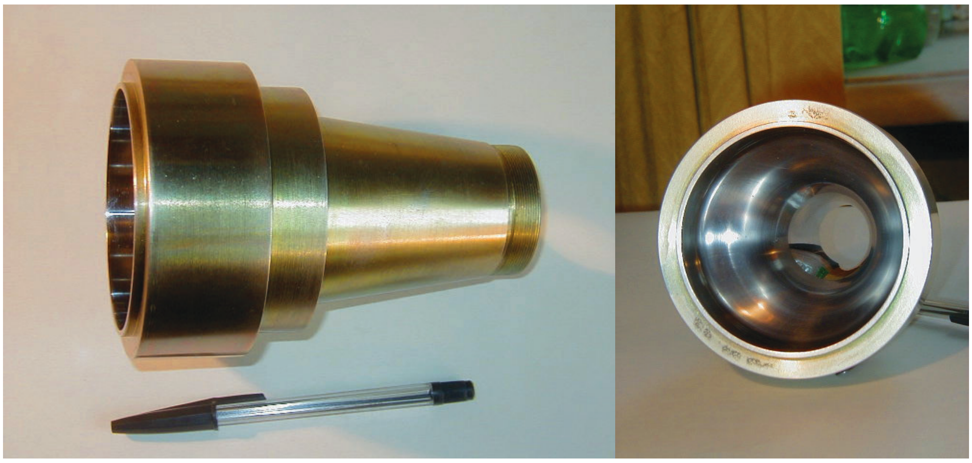

Figure 2. Photograph of the contoured convergent nozzle $M_a = 1$ in two projections (the nozzle exit radius is $R_a = 15$ mm).

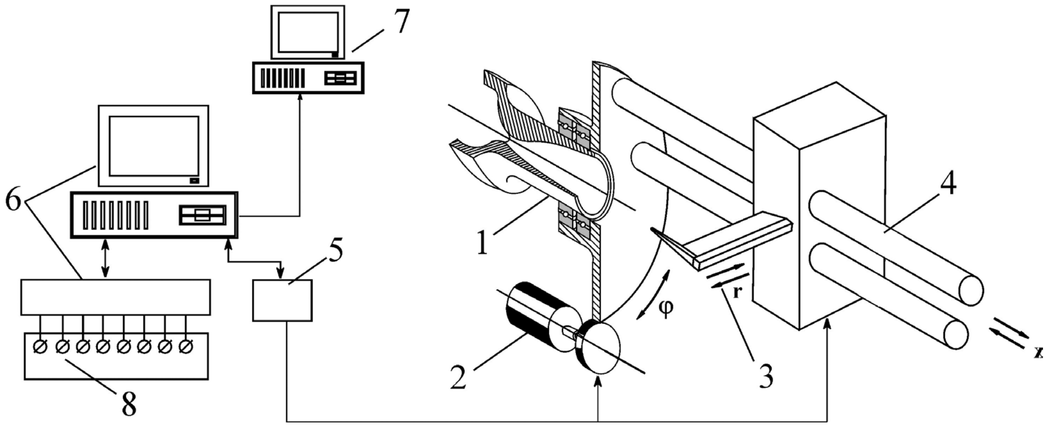

Figure 3. Chart of measurements on the jet module of the T-326 hypersonic wind tunnel with the use of the PCI-1710HG multifunctional board and sketch of the traversing gear with the nozzle: 1- nozzle, 2 - device for azimuthal motion, 3 - device for radial motion, 4 - device for streamwise motion, 5 - panel for controlling the traversing gear, 6 - automated system for data acquisition (PC, Advantech multifunctional board), 7 - panel for controlling wind-tunnel actuation and maintaining the working regime in the T-326 wind tunnel, 8 - primary sensors.

Figure 3 shows a diagram of measurements in the jet module of the T-326 wind tunnel.

The data acquisition system 6 allows manual and automatic control of the traversing gear motion along the coordinates and polling of sensors measuring flow parameters (pressure and temperature in the settling chamber of the jet module) with an Advantech multifunctional board. The flow parameters were fed to an external computer 7 for precise maintaining of the gas-dynamic flow regime. The outer diameter of the total pressure probe (Pitot tube) was 0.6 mm.

Availability of an automated data acquisition system, nozzles with a high-quality inner surface, piezoresistive pressure transducers, and a program for data acquisition and processing made it possible to perform experiments to study the effect of controlled disturbances generated in the shear layer of the jet and to reveal their topological structure and the character of their spatial evolution.

3. ANALYSIS OF EXPERIMENTAL DATA

3.1 Supersonic jet exhausting from a nozzle with single chevron at the exit

The experimental studies of the influence of a single chevron on the flow structure in a supersonic jet were performed in the jet module of the T-326 wind tunnel. A supersonic jet exhausted from a convergent nozzle with a vortex generator shaped as a single triangular chevron.

The gas-dynamic parameters of the jet were determined by the geometric Mach number at the nozzle exit, which was equal to $M_a = 1.0$, and by the nozzle pressure ratio $n_p = P_a/P_c = 2.64$ (P_a is the pressure at the nozzle exit and $P_c = 0.1$ MPa is the pressure in the test section of the facility). The Reynolds number based on the flow parameters and the nozzle exit diameter was $\mathrm{Re}_d = 2.3{\cdot}10^6$. A constant pressure ratio $N_{pr} = P_0/P_c = 5$ (P_0 is the pressure in the settling chamber of the jet module) was maintained during the experiment. The chevron was attached to the nozzle exit so that the chevron surface was a continuation of the inner surface of the nozzle (see Figure 4) and was shaped as an isosceles triangle with a base of 4 mm and a height of 8 mm.

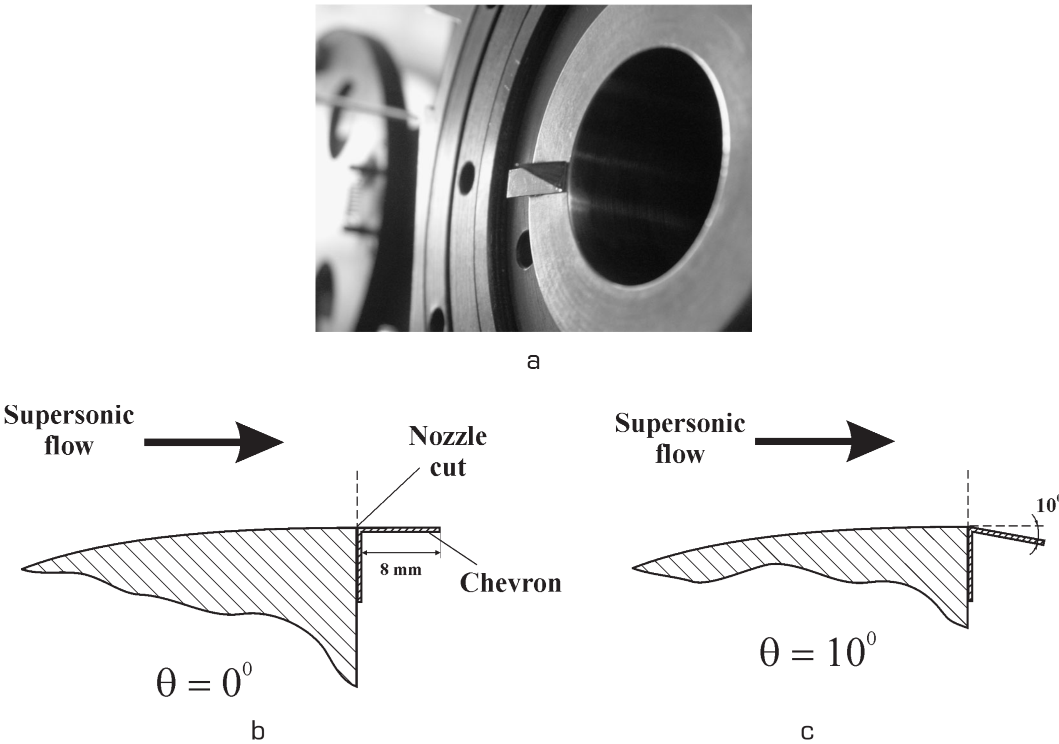

Figure 4. Nozzle with a single chevron: a – photograph of the nozzle with the chevron at $\theta = 0°$, *b*, *c* – possible angles of chevron alignment

The angle of chevron inclination θ with respect to the generatrix of the inner surface of the nozzle at the exit could have two values: $\theta = 0°$ or 10° (see Figure 4, b, c). The angle $\theta = 0°$ coincided with the continuation of the generatrix of the inner surface of the nozzle; the angle $\theta = 10°$ corresponded to chevron deflection from the jet axis, such that the chevron generatrix was directed over the tangent to the jet boundary.

Figure 5 shows a schlieren photograph and a sketch of the initial section of a supersonic underexpanded jet exhausting from the nozzle with the chevron angle $\theta = 0$. The schlieren image (Figure 5,a) clearly shows the shock-wave structure of the flow at the initial section of the supersonic underexpanded jet; the chevron is also visible (dark triangle in the middle of the picture).

A supersonic underexpanded jet exhausting from an axisymmetric nozzle into an ambient space is characterized by substantially nonuniform distributions of gas-dynamic quantities both along the axis and in the transverse direction [14]. The pressure at the nozzle exit in the underexpanded jet is higher than the ambient pressure; therefore, the velocity vector of the supersonic jet flow has a radial component directed away from the axis. For this reason, the jet boundary acquires a barrel-type shape at the initial segment, which leads to formation of a barrel shock near the nozzle exit; a triple configuration of shock waves with a Mach disk is formed owing to reflection of this barrel shock from the axis.

The streamlines near the supersonic underexpanded jet boundary are curved. The magnitude of this curvature depends on the exhaustion conditions and on the geometry of the nozzle exit section: Mach number, pressure difference at the nozzle exit, and initial state of the boundary layer of the jet.

Azimuthal variations of the total pressure registered by the Pitot tube are induced by the presence of streamwise vortices in the shear layer, whose formation and evolution are promoted by the “negative curvature” of streamlines [6]. The latter is usually associated with the Taylor-Goertler hydrodynamic instability in the shear layer of the supersonic underexpanded jet.

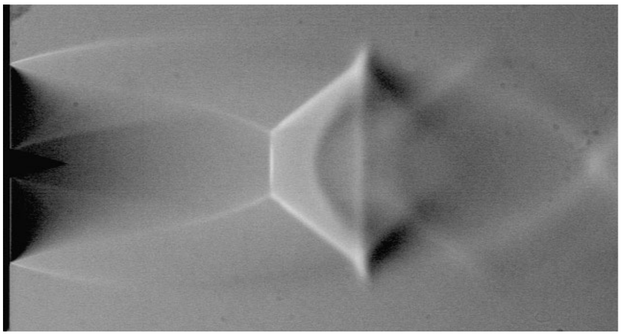

a

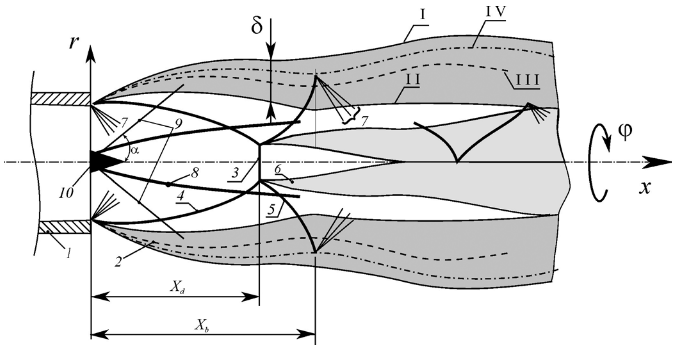

b

Figure 5. Schlieren photograph (a) and flow structure (b) at the initial section of a supersonic underexpanded jet $M_a = 1$, $n_p = 2.64$ in the presence of a chevron: 1 – nozzle ($R_a = 15$ mm); 2 – shear layer (the inner and outer boundaries are indicated by I and II, the middle of the shear layer is indicated by III, and the line of the constant Mach number M = 1 is indicated by IV); 3 – Mach disk; 4, 5 – barrel and reflected shock waves; 6 – shear layer formed behind the point of intersection of the shock waves 3,4,5; 7 – expansion fan, 8 – wake behind the chevron, 9 – Mach waves, 10 – chevron, x_b – length of the first barrel of the jet, x_d – distance from the nozzle exit to the Mach disk.

The flow structure formed by chevron interaction with the supersonic jet flow is illustrated in Figure 5,b, which shows typical elements of the supersonic underexpanded jet structure: expansion wave, barrel shock wave, Mach disk, and shear layer formed behind the triple point. Additional elements of the jet structure formed owing to the chevron presence are the wake behind the chevron *8* (Fig 5,b) and weaker perturbations corresponding to the Mach waves propagating in the supersonic part of the shear layer of the jet (9).

The experiment was performed as follows. After a given pressure P_0 was reached in the settling chamber of the jet module of the wind tunnel and the position of the total pressure probe (Pitot tube) with respect to the streamwise axis x was fixed, the radial pressure profiles $P_t(r)$ were measured. After that, the streamwise x and radial r coordinates were fixed, and the azimuthal distribution of pressure $P_t(\varphi)$ was measured as a function of the azimuthal angle. The Pitot tube was moved over the radius with a step of 0.2 mm and over the angle with a step of 1˚. The probe was moved by an automated traversing gear in three directions: along the streamwise x, transverse r, and azimuthal φ coordinates.

Typical radial profiles of the measured total pressure for the undisturbed (“clear”) jet and for the jet with the chevron in two angular positions ($\theta = 0˚$ and 10˚) are plotted in Figure 6.

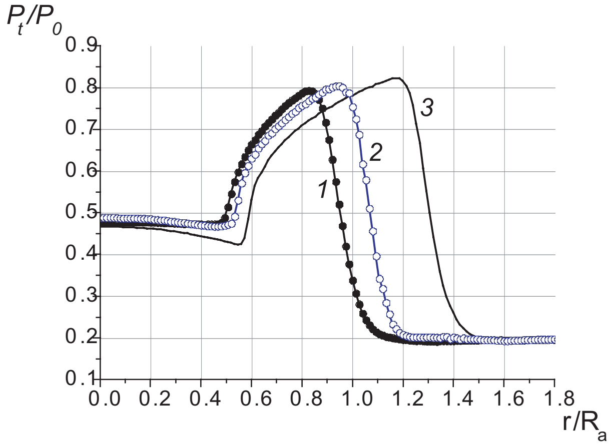

Figure 6. Radial profiles of pressure in the jet cross section 1 - $\theta = 0°$, $\varphi = 0°$, 2 - $\theta = 10°$, $\varphi = 0°$, 3 - undisturbed jet

The pressure distributions $P_t(r)$ were measured in the plane of the chevron axis ($\varphi = 0°$). The inner boundary of the shear layer of the jet corresponds to the pressure peak on the profile. In the presence of the chevron, the inner boundary is shifted toward the jet axis (curves 1 – 2). The outer boundary of the jet for the chevrons with $\theta = 0°$ and $10°$, which corresponds to the radius $r/R_a = 1.5$ on the profile, is also shifted toward the jet axis. The greatest deformation of the jet boundary is observed if the chevron is "submerged" into the jet with $\theta = 0°$. The angle of deflection of the jet boundary at the nozzle exit in the expansion wave at $N_{pr} = 5.0$ is 17° (angle of flow deflection in the Prandtl-Meyer flow). Therefore, if the plane of the vortex generator (chevron) is aligned at 0°, then the angle between the flow direction and the chevron is equal to 17°. For the chevron mounted at 10°, the angle of chevron-flow interaction is 7°, i.e., weaker interaction is expected. This fact is confirmed by the data in Figure 6. The difference of the pressure profile 2 corresponding to $\theta = 10°$ from the undisturbed jet profile 3 is smaller than that in the case with $\theta = 0°$.

The azimuthal distributions of the normalized pressure at a distance $x/R_a = 2.0$ from the nozzle exit for different positions of the Pitot tube are shown in Figure 7 for the chevrons aligned at $\theta = 0°$ and 10°. At $\varphi = 0°$, the azimuthal profiles have the minimums of the measured total pressure. The pressure minimum at $\varphi = 0°$ corresponds to the chevron axis and is caused by the wake behind the chevron and by the formation of two large-scale streamwise vortex structures.

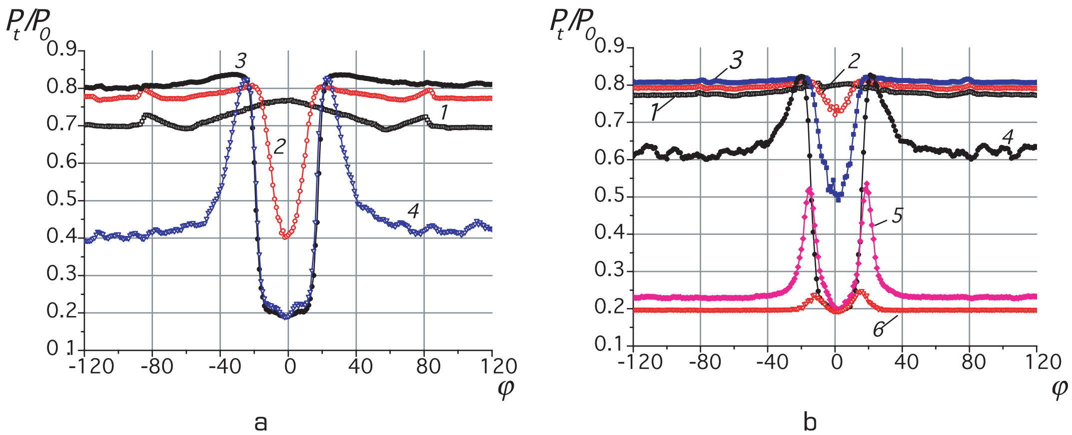

Figure 7. Azimuthal distributions of pressure in the jet cross section $x/R_a = 2.0$: a - angle of chevron inclination $\theta = 0°$, 1 - $r/R_a = 0.73$, 2 - $r/R_a = 0.93$, 3 - $r/R_a = 1.2$, 4 - $r/R_a = 1.33$; b - angle of chevron inclination $\theta = 10°$, 1 - $r/R_a = 0.93$, 2 - $r/R_a = 1.0$, 3 - $r/R_a = 1.07$, 4 - $r/R_a = 1.27$, 5 - $r/R_a = 1.4$, 6 - $r/R_a = 1.6$

In the compressed layer of the supersonic underexpanded jet, in addition to the main disturbance in the form of the wake, there are also symmetric maximums of pressure at certain values of the radius at

φ = +80° and φ = -80° (curves 1, 2 in Figure 7,a). The magnitude of these maximums is rather small. This value of the radius corresponds to supersonic velocities in the jet flow. These comparatively weak perturbations induced by formation of shock waves ahead of the chevron and propagating in the supersonic jet flow are interpreted as the Mach waves (Figure 5,b).

The chevron aligned at θ = 10˚ generates less intense disturbances in the main jet than the chevron aligned at θ = 0˚ (Figure 7,b): the main effect caused by the wake behind the chevron is manifested as a pressure minimum at φ = 0˚. Weak perturbations of the Mach wave type are actually not registered at x/R_a = 2.0.

At the jet periphery, the azimuthal pressure profile is transformed, and two symmetric local maximums of pressure are formed: curve *4* in Figure 7,a, φ = 25˚; curves 5, 6 in Figure 7,b. The origin of the secondary maximum is associated with formation of mushroom-shaped structures in the shear layer and will be discussed in more detail below, where the results of numerical simulations of the jet flow are described (Section 4).

Zapryagaev and Kiselev [15] published the results of an experimental study of the flow structure in a supersonic underexpanded jet with injection of a single transverse microjet with variable geometric and gas-dynamic parameters. This microjet was injected from a micronozzle 1.5 mm in diameter near the exit of the basic nozzle.

To compare the effect of various vortex generators on the jet flow, we consider the azimuthal profiles of the total pressure for the jet with the microjet ($Npr_j = P_{0j}/P_c$ = 4.44, P_{0j} is the stagnation pressure in the micronozzle) and with the chevron aligned at θ = 0° (see Figure 8). The data were obtained in the compressed layer of the supersonic underexpanded jet in the cross section r/R_a = 1 at identical gas-dynamic parameters of the jet (M_a = 1.0, n_p = 2.64).

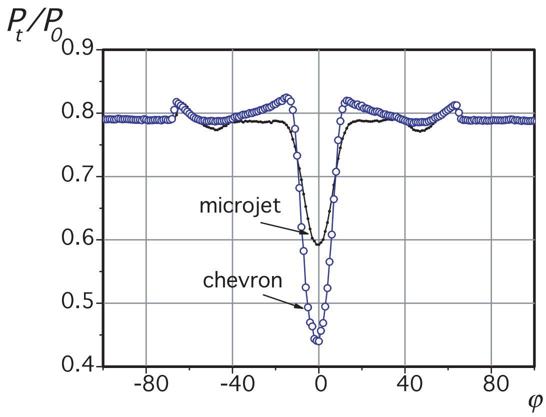

Figure 8. Azimuthal profiles of pressure for a nozzle with a chevron and a microjet; x/R_a = 1.5, r/R_a = 1.0.

The pressure minimum at φ = 0˚ on the profile corresponds to the axial position of the microjet and the chevron. It is seen from the figure that the chevron exerts a more intense effect than the microjet at Npr_j = 4.44.

Injection of a microjet, like installation of a chevron, induces disturbances of the Mach wave type: at φ = ± 50˚, such disturbances (Mach waves) are observed in the supersonic part of the shear layer of the jet. The coincidence of the additional maximums for the both types of artificial disturbances means that the perturbations generated by both the chevron and the microjet propagate at the same angle.

Disturbances of the Mach wave type propagate at the angle α: $\sin\alpha = \frac{1}{M}$ (M is the local Mach number). The calculated Mach angle is α = 33.5° and corresponds to the Mach number M= 1.81. This value is close to the jet Mach number calculated by the formula for isentropic expansion of the jet up to the ambient pressure, which was

$$M_j = \sqrt{\frac{2}{\gamma-1}\left[\left(\frac{P_o}{P_c}\right)^{\frac{\gamma-1}{\gamma}}-1\right]} \tag{1}$$

maintained constant and equal to $M_j = 1.71$ in the experiment.

3.2. Set of chevrons

The spatial structure of a supersonic underexpanded jet exhausting from a convergent nozzle with special vortex generators (chevrons) at the exit was experimentally studied. The supersonic underexpanded jet exhausted into the ambient space (air) from an axisymmetric convergent contoured nozzle with $M_a = 1$, equipped with a cylindrical insert with six chevrons. The gas-dynamic parameters of the jet were the same as in the experiment with a single chevron. A sketch of the nozzle with chevrons is shown in Figure 9. The radius of the nozzle and the insert with chevrons at the exit was $R_a = 15$ mm. The chevrons were located with an identical step over the radius and were shaped as trapezoids with a height of 10 mm and base lengths of 7 and 4.5 mm. The generatrix of the inner surface of the chevron was a continuation of the inner surface of the nozzle.

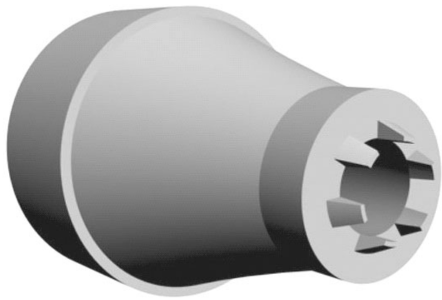

Figure 9. Sketch of a convergent nozzle with chevrons.

Figure 10 shows the schlieren pictures of the initial section of a supersonic underexpanded jet exhausting from a "clear' nozzle and from a nozzle with chevrons at the exit. The schlieren pictures were obtained by an optical visualization system consisting of an IAB-451 shadowgraph and a digital camera.

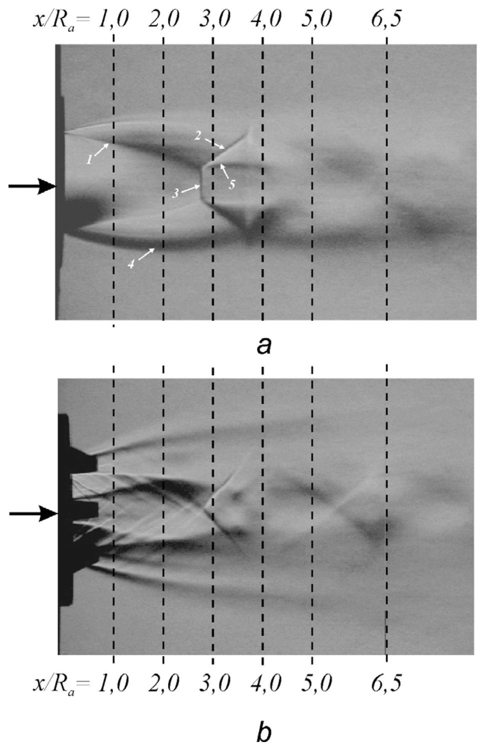

Figure 10. Schlieren photographs of a supersonic underexpanded jet with $M_a = 1.0$, $n_p = 2.64$ exhausting from a "clear" nozzle (a) and from a nozzle with chevrons at the exit (b).

For the free supersonic underexpanded jet, a typical shock-wave structure (see Figure10,a) includes the barrel shock wave *1*, the reflected shock wave *2*, the Mach disk *3*, the jet boundary *4*, and the shear layer *5* formed behind the triple point of intersection of the shock waves *1, 2, 3*. In the jet exhausting from the nozzle with chevrons (see Figure10, b), the pattern of gas exhaustion is more complicated: the jet boundary becomes smeared, the chevrons interact with the supersonic jet flow, which leads to formation of a series of shock waves interacting with each other.

Radial and azimuthal profiles of pressure were obtained in the jet cross sections x/R_a = 1.0, 2.0, 3.0, 4.0, 5.0, and 6.5. Typical radial profiles of the pressure distribution in various cross sections of the jet are shown in Figure 11. In the "clear" jet, a drastic increase in pressure corresponding to the barrel shock location is registered at r/R_a = 0.6, x/R_a = 2.0 (see Figure 11,b). The pressure maximum P_t/P_0 =

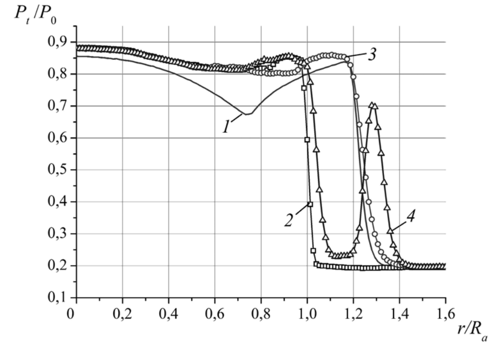

a

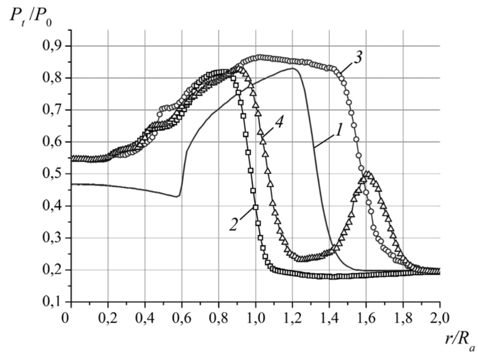

b

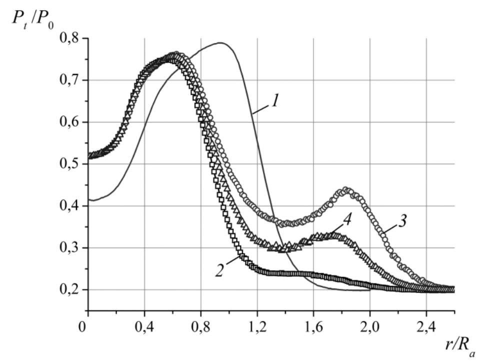

c

Figure 11. Radial profiles of pressure measured in different cross sections of the jet: *a* – x/R_a = 1, *b* – x/R_a = 2, *c* – x/R_a = 5; *1*- jet exhausting from a "clear" nozzle; *2* – *4* – jet exhausting from a nozzle with chevrons for different azimuthal positions of the Pitot tube corresponding to the radial displacement lines: *2*- with respect to the chevron axis (φ = 0°), *3*- between two neighboring chevrons (φ = 30°), *4*- in the section at φ = 15°

0.825 (r/R_a = 1.2) corresponds to the inner boundary of the shear layer of the jet, and the pressure minimum Pt/P_0 = 0.2 (r/R_a = 1.6) corresponds to the pressure on the outer boundary of the jet.

Interaction of chevrons with the supersonic flow at the initial section of the jet forms a complicated shock-wave structure with additional shock waves interacting with each other.

The presence of chevrons (curves *2 – 4*) substantially changes the shock-wave structure of the supersonic underexpanded jet. For instance, wavy variations of pressure are observed in the jet cross section x/R_a = 2.0 (Figure 11,b) owing to the presence of shock waves formed by jet interaction with chevrons and intersecting on the axis. The pressure on the jet axis becomes higher than that in the undisturbed jet, and this difference increases with distance from the nozzle exit.

The boundaries of the shear layer of the jet exhausting from the nozzle with chevrons are changed: the inner boundary of the jet is shifted toward the axis opposite the chevron and away from the axis between the chevrons. The outer boundary located between the neighboring chevrons (curve 3) is also shifted away from the axis. As a result, the transverse size of the jet in the region between the chevrons increases. Considerable deformation of the boundary opposite the chevron is caused by inflow of a low-pressure gas from the ambient medium. At additional maximum of pressure is registered at an angle φ = 15° (curve 4); this maximum is caused by formation of mushroom-shaped structures and is analyzed in more detail below. The barrel shock wave is not registered in the jet exhausting from the nozzle with chevrons. With distance from the nozzle exit (Figure 11,c), the inner boundary of the shear layer is shifted toward the axis of a comparatively undisturbed flow, whereas the outer boundary of the jet moves away from the axis.

Figure 12 shows typical azimuthal profiles of the normalized pressure in the jet cross sections x/Ra= 2 and 4. The measurements were performed in the range of the angles $\varphi = 0 \div 360°$. For better presentation of the spatial flow in the shear layer of the jet, however, the results are given for the range $\varphi = 0 \div 180°$.

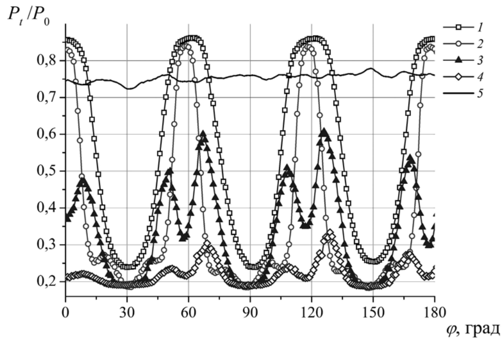

a

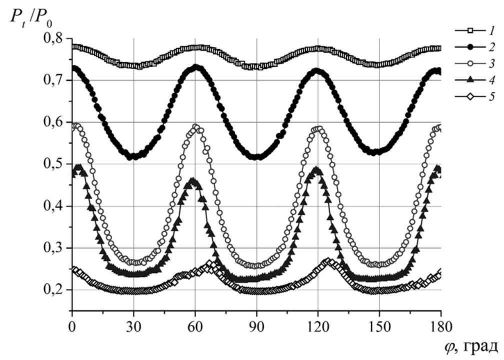

b

Figure 12. Azimuthal distributions of the normalized pressure measured in different cross sections of the jet: *a* - x/R_a = 2.0 (*1*- r/R_a = 1.0, *2*- r/R_a = 1.27, *3*- r/R_a = 1.6, *4*- r/R_a = 1.73, *5*- r/R_a = 1.27 (undisturbed jet)), *b* - x/R_a = 4.0 (*1*- r/R_a = 0.67, *2*- r/R_a = 0.8, *3*- r/R_a = 1.0, *4*- r/R_a = 1.27, *5*- r/R_a = 2.13)

In the undisturbed jet (curve *5* in Figure 12,a), there are azimuthal inhomogeneities of pressure owing to natural roughness on the inner surface of the nozzle.

The chevrons induce significant transformations of the spatial distributions of gas-dynamic parameters. The minimum values of pressure are registered at the values of φ corresponding to the wake behind the chevron. The minimum values of pressure are commensurable with the pressure in the test section of the jet module. Additional maximums of pressure appear on the outer boundary of the jet (curve 3 in Figure 12,*a*) inside the shear layer, as in experiments with a single chevron. The magnitude of these maximums decreases with a further increase in the jet radius (curve 4 in Figure 12,a). The emergence of the minimums and maximums is caused by large-scale streamwise vortices resulting from interaction of the chevrons with the supersonic jet flow. Transformation of the minimums with formation of additional maximums does not occur at large distances from the nozzle exit (Figure 12,b).

Figure 13 shows the experimentally measured azimuthal distributions of the Pitot pressure in various cross sections of the jet exhausting from the nozzle with chevrons.

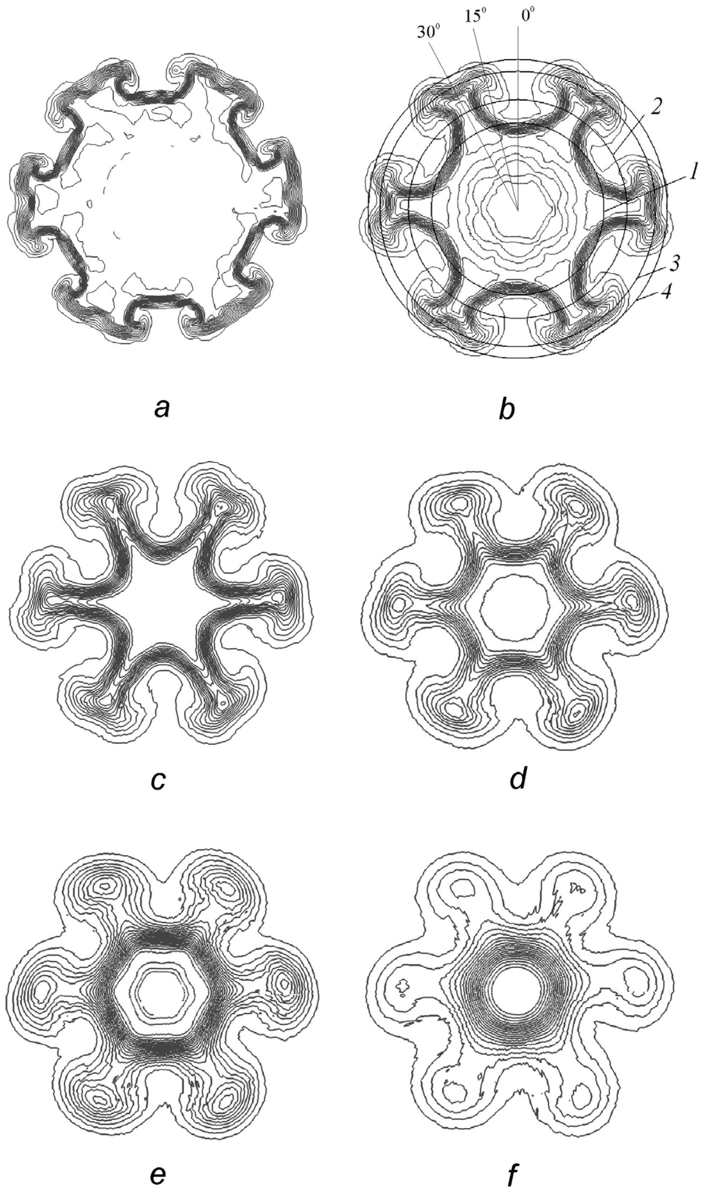

Figure 13. Contours of pressure measured in different cross sections of the jet: *a*- $x/R_a = 1.0$, *b*- $x/R_a = 2.0$, *c*- $x/R_a = 3.0$, *d*- $x/R_a = 4.0$, *e*- $x/R_a = 5.0$, *f* - $x/R_a = 6.5$; *1*- $r/R_a = 1.00$, *2*- $r/R_a = 1.27$, *3*- $r/R_a = 1.60$, *4*- $r/R_a = 1.73$

Thirty to thirty eight azimuthal distributions of pressure were obtained in each cross section. Thus, the results measured at 10,800 to 13,600 points were used to construct the flow topology in each cross section of the jet. The azimuthal angles $\varphi = 0$, 15, and 30° shown in Figure 13,b correspond to the radial lines on which the pressure profiles plotted in Figure 11 were obtained. The numbers *1 – 4* indicate the radii at which the azimuthal pressure profiles in Figure 12,a were measured.

The resultant flow structure is induced by formation of large-scale vortex structures owing to interaction of the chevrons with the jet boundary. Each chevron generates a pair of oppositely rotating streamwise vortices. It is seen that the vortex structures have a mushroom shape. The process of generation, evolution, and dissipation of artificially induced mushroom-shaped disturbances is clearly traced. The generation is observed at $x/R_a = 1$, the evolution occurs at $x/R_a = 2 \div 3$, and the dissipation is observed at $x/R_a = 6.5$. The vortex flow behind the chevron ($\varphi = 0°$) is directed so that the low-pressure gas enters the jet in the radial direction (see Figure13,b). In the region between the neighboring chevrons ($\varphi = 30°$), the high-pressure gas is entrained to the gas periphery.

The emergence of the secondary pressure maximum at $r/R_a = 1.6$, $\varphi = 15°$ (see Figure 11,b) can be explained by using isobars in the jet cross section (curve *3* in Figure 13,b). A high-pressure reverse vortex flow directed toward the jet axis is registered at $\varphi = 15°$, $r/R_a = 1.6$.

With distance from the nozzle exit ($x/R_a = 5.0$ and 6.5), the ordered flow structure becomes smeared, the vortex flow intensity decreases, the "stems" of the mushroom-shaped structures become thinner, the pressure decreases, and the vortex is separated from the jet core (see Figure 13,f). It should be noted that the mushroom-shaped structures exist at a rather large distance from the nozzle exit.

4. NUMERICAL CALCULATIONS

4.1 Undisturbed jet

The numerical study was performed with the use of the Fluent commercial software system. Exhaustion of a supersonic underexpanded jet into a semi-infinite space was considered. Stationary axisymmetric Navier-Stokes equations were solved with the use of the k-ω SST turbulence model. The flow parameters used in the numerical study were close to the experimental values: total pressure corresponding to the pressure in the settling chamber $P_0 = 0.5$ MPa, total temperature corresponding to the stagnation temperature in the settling chamber $T_0 = 298$ K, Mach number at the nozzle exit $\mathrm{M}_a = 1.0$, ambient pressure $P_c = 0.1$ MPa, and ambient temperature $T_c = 298$ K. A rectangular grid was used in the computations. The solution was obtained with the use of the second-order difference scheme for calculating the flow parameters and the first-order scheme for calculating the turbulence parameters.

A schlieren picture of the supersonic underexpanded jet is shown in Figure 14 (on the top). The flow direction is from left to right. The gas-dynamic structure of the initial part of the jet is characterized by the presence of shock waves, expansion waves, and shear layer. The lower part of Figure 14 shows the density isolines obtained by numerical simulations of the supersonic underexpanded jet with gas-dynamic parameters at the nozzle exit close to experimental values.

The spatial flow structure (locations of the Mach disk, barrel and reflected shock waves, and jet boundaries) visible in the schlieren picture is in good agreement with numerical results.

The radial distributions of the normalized total pressure measured by the Pitot tube in the range from $x/R_a = 0.067$ to $x/R_a = 7.0$ are compared in Figure 15 with the numerical results. As the total pressure in measured by the Pitot tube in the experiment, the numerical data have to be converted to a form suitable for comparisons with the experimental results. The calculated static pressure p and the local Mach number M_x in the x direction were used to recalculate the pressure distributions Pt/P_0 by the formulas given in [16]:

$$P_t / P_0 = \begin{cases} \dfrac{p}{P_0}\left(1+\dfrac{k-1}{2}\mathrm{M}_x^2\right)^{\frac{k}{k-1}}, \mathrm{M}_x < 1, \\ \dfrac{p}{P_0}\left(\dfrac{2k}{k+1}\mathrm{M}_x^2-\dfrac{k-1}{k+1}\right)\left(\dfrac{4k}{(k+1)^2}-\dfrac{2(k-1)}{(k+1)^2\mathrm{M}_x^2}\right)^{\frac{-k}{k-1}}, \mathrm{M}_x \geq 1. \end{cases}, \qquad (2)$$

Here, p is the static pressure, M_x is the local flow Mach number along the jet axis x, and $k = 1.4$ is the ratio of specific heats of air. The upper expression is the formula for isentropic flow (which was used to calculate the total pressure in a subsonic flow). The lower expression is the Rayleigh formula (which was used to calculate the total pressure behind the normal shock wave in a supersonic flow).

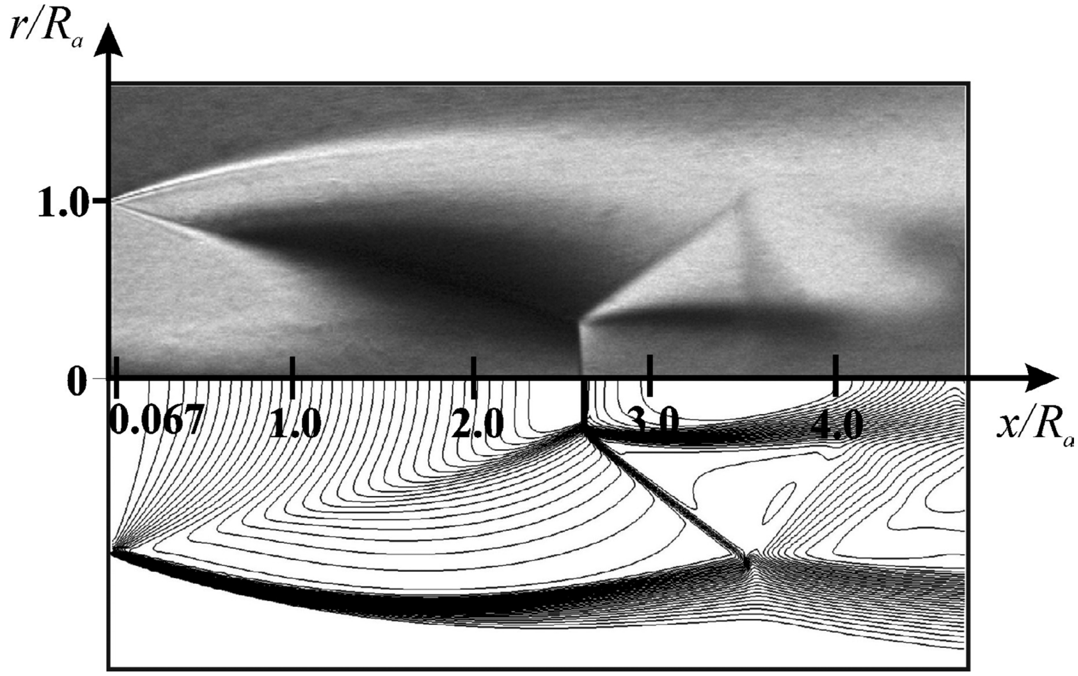

Figure 14. Schlieren photograph of the initial section of a supersonic underexpanded jet with the Mach number at the nozzle exit M_a = 1.0 and the nozzle pressure ratio n_p = 2.64 (upper figure); density contours plotted on the basis of results of numerical simulations (lower figure).

The experimental and calculated data within the first barrel of the jet (x/R_a = 0.067 – 4.0) are in reasonable agreement. The calculated data predict the basic features of the stationary structure of the supersonic nonisobaric jet. The measured and numerical pressures on the jet axis coincide with each other. The locations of the barrel shock waves registered in the region of the jump-like increase in pressure on the profiles at x/R_a = 1.0, 2.0, and 3.0 (P_t/P_0 = 0.8, 0.6, and 0.4) are in reasonable agreement. The pressure maximum P_t/P_0 = 0.9 on the profile x/R_a = 3.0 (r/R_a = 0.56) corresponds to passage of the Pitot tube through the flow region between the shear layer emanating from the triple point and behind the reflected shock wave.

The greatest differences between the experimental and numerical data are observed in the shear layer. The shear layer in Figure 15 is registered as a region with a strong pressure gradient whose magnitude decreases with increasing distance from the nozzle exit. The calculated shear layer thickness is somewhat smaller than that recorded in the experiment. Apparently, this is caused by streamwise vortex structures in the shear layer [2], which exert a significant effect on the turbulent mixing processes. Because of the axisymmetric character of the solution, it is not possible to take into account the influence of the streamwise vortex structures of the Taylor-Goertler type observed in experiments. The initial level of turbulence in the experiments was assumed to be ~ 1%.

4.2. Jet with chevrons

A numerical study was performed with the use of the Fluent software system for the problem of exhaustion of a supersoniuc nonisobaric jet to refine the gas-dynamic structure and to obtain quantitative data in the supersonic jet in the presence of vortex-forming devices (tabs or chevrons) at the nozzle exit. Three-dimensional Navier-Stokes equations were solved with the use of the (k-() turbulence model.

The calculations were performed for a nozzle with the exit radius Ra=15 mm with six chevrons at the nozzle exit (see Figure 9). The Mach number at the nozzle exit was __= 1, the nozzle pressure ratio was np= 2.64, and the Reynolds number based on the nozzle-exit diameter d was Red= 2.3·106. The computational domain was a segment whose size was 1/12 of a cylinder of length x/Ra= 5.0 and radius r/Ra= 3.33 (see Figure 16). The side planes of the segment are planes of symmetry of the problem; one of them passes through the middle of the chevron, and the other is at an identical distance from the neighboring chevrons.

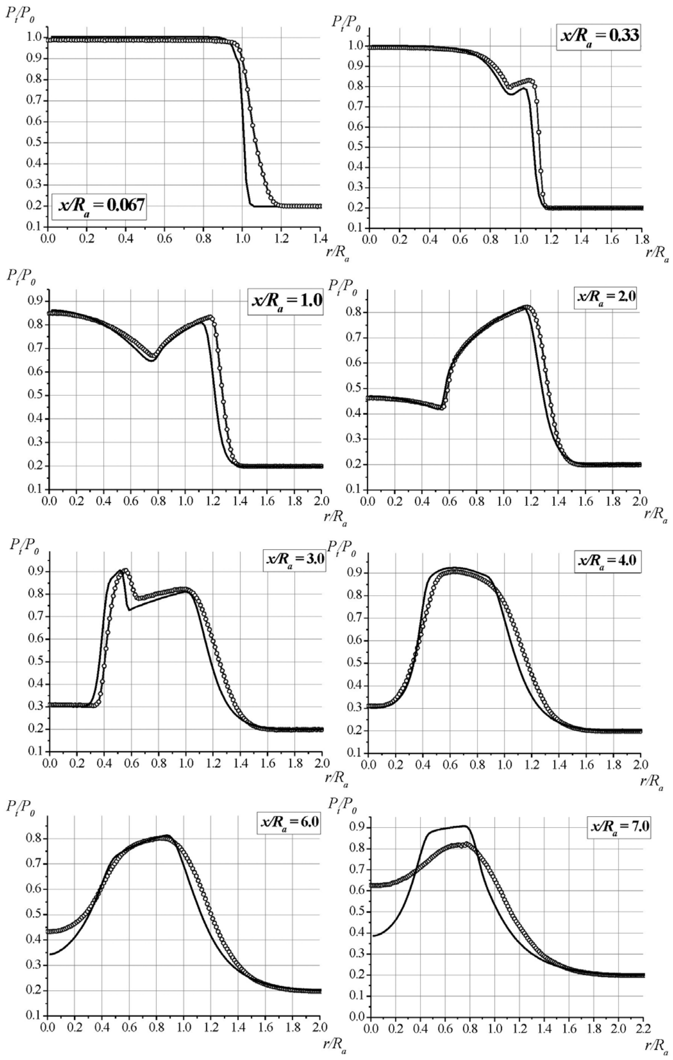

Figure 15. Radial profiles of the measured total pressure (circles) and profiles obtained in numerical simulations (solid curve) at the initial section of a supersonic underexpanded jet with $M_a = 1.0$.

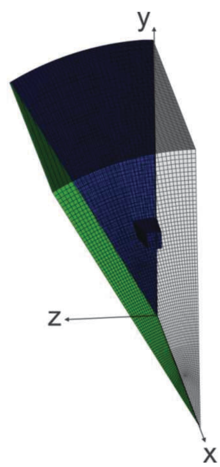

Figure 16. Computational grid

To estimate the reliability, the calculated data were compared with the results of an experiment performed under the same geometric and gas-dynamic conditions. Figure 17 shows the radial distributions of the pressure P_t/P_0 in the jet cross section $x/R_a = 1$ at different angles of the angle φ. The pressure distributions along the radial line passing through the middle of the chevron at $\varphi = 0°$ (see Figure 17,a), along the line at $\varphi = 15°$ (see Figure 17,b), and along the line passing at an identical distance between the neighboring chevrons at $\varphi = 30°$ (see Figure 17,c) are plotted.

It is seen in Figure 17 that the experimental and calculated data are in reasonable agreement. The greatest difference is observed at $\varphi = 15°$, $r/R_a = 1.3$ (see Figure 17,b) corresponding to the secondary maximum of pressure. The calculated and measured values of pressure in the flow core are in good agreement. The agreement in the shear layer of the jet is only qualitative, because the turbulence model used in the calculations allowed us to obtain a qualitative description of the physical model of the flow, but could not reproduce all elements of the flow.

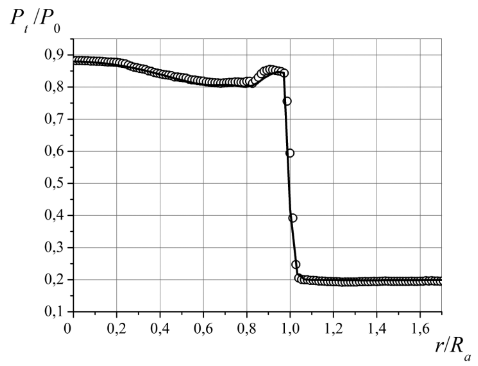

a

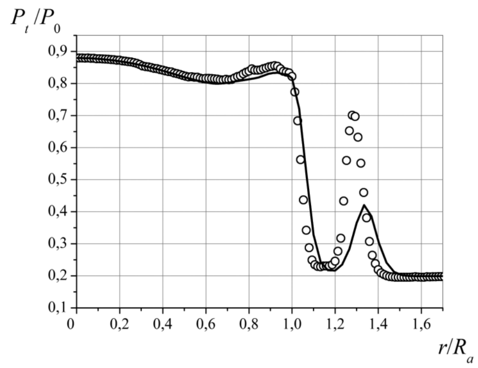

b

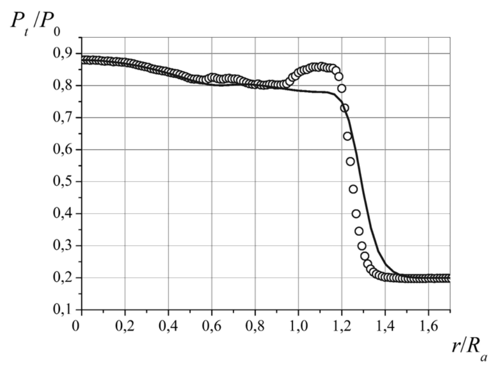

c

Figure 17. Radial profiles of pressure in the jet cross section $x/R_a = 1.0$ for different values of φ: The curves show the results calculated by Eqs. (2); the points are the experimental data; *a*- $\varphi = 0°$, *b*- $\varphi = 15°$, *c*- $\varphi = 30°$.

Figure 18,a shows the calculated contours of the Pitot pressure for the sector 30˚≤φ≤30˚. A mushroom-shaped structure generated by the chevrons located on the left and on the right of it is seen. Figure 18, b shows the azimuthal distributions of the Pitot pressure for the radii r/R_a =1.00, 1.27, 1.60, and 1.73 shown in Figure 18,a. The lines passing through the "stem" of the mushroom-shaped structure (r/R_a =1.00 and 1.27) have one maximum, and those that pass through the "cap" (r/R_a = 1.60 and 1.73) have a double maximum. Registration of the double maximum is ensured by the total pressure gradient generated by the vortex-forming forces that turn the gas flow from under the chevrons (planes φ = -30˚ and φ = 30˚) toward the plane of symmetry between the chevrons (plane φ = 0˚, to the "stem" of the mushroom-shaped structure) and then back toward the planes of symmetry of the chevrons (φ = -30° and φ = 30°) but above the latter. This distribution of the Pitot pressure is also typical for a nozzle with one chevron (curve 4 in Figure 7,a and curves 5, 6 in Figure 7,b) and with six chevrons (Figure 12,a, double maximum on curves 3, 4); the pressure minimum corresponds to the area near the chevron.

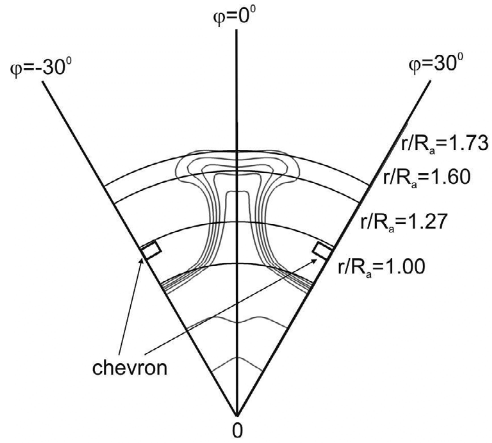

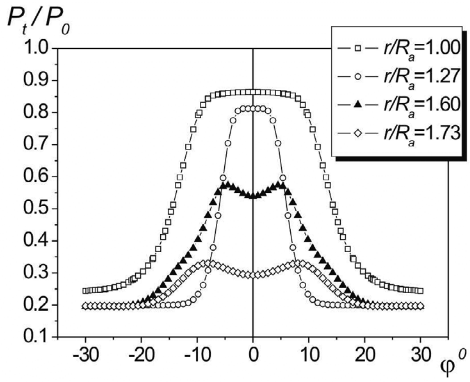

Figure 18. Total pressure contours (a) and azimuthal distributions of pressure (b) obtained in numerical simulations.

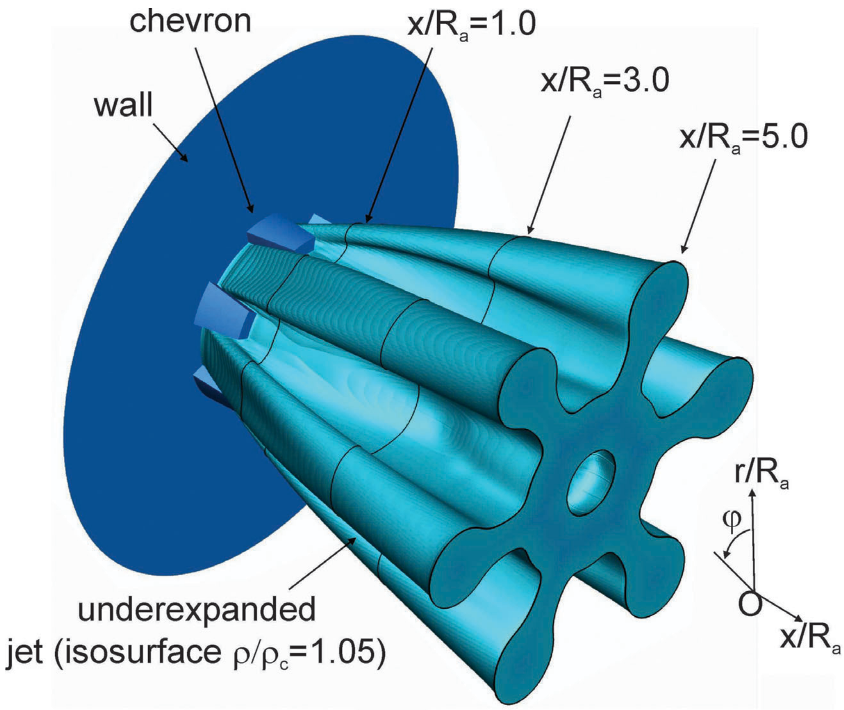

Figure 19. General view of the jet: the outer surface of the jet is formed by the surface ρ/ρ_c = 1.05, where ρ is the density of air and ρ_c is the density of air in the undisturbed area.

The spatial flow structure reconstructed in the calculations is illustrated in Figure 19, which shows the distribution of the air density in the case of jet exhaustion from the nozzle with chevrons. The mushroom-shaped structure of the flow obtained in the experiment is clearly visible.

Figure 20 shows the streamlines constructed on the basis of the radial and azimuthal components of the velocity vector. Each chevron generates a pair of vortices formed near the side surface of the chevron and propagating in the downstream direction. The flow has a mushroom-shaped structure and consists of six paired vortices, which agrees qualitatively with the experimental data (see Figure 13). The transverse size of the vortices increases with distance from the nozzle exit, and their intensity decreases. The computations predict an additional layer of vortices in the cross section $x/R_a = 5$ (Figure 19,c). The scale of these additional vortices is much smaller than the scale of the primary vortices.

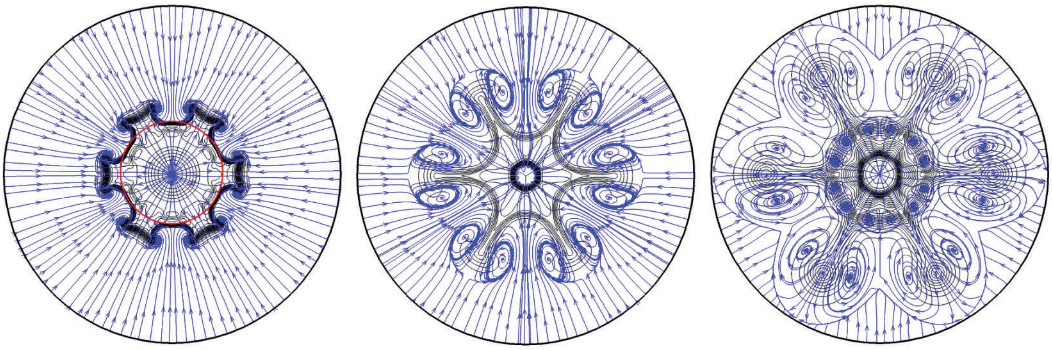

a b c

Figure 20. Streamlines constructed on the basis of the radial and azimuthal components of the velocity vector in the jet cross section: *a* – $x/R_a = 1.0$, *b* – $x/R_a = 3$, *c* – $x/R_a = 5$.

5. CONCLUSIONS

An experimental study of the flow structure at the initial section of a supersonic axisymmetric underexpanded jet exhausting from a convergent nozzle was performed with the use of a high-accuracy automated system of data acquisition and processing. Numerical simulations ensured reasonable agreement with experimental data.

Disturbances of two types are observed during interaction of a single chevron and the main jet. The stronger disturbance is caused by the presence of the wake component and by generation of two streamwise vortices. The weaker disturbance is manifested in the form of perturbations of the Mach wave type propagating in the supersonic part of the shear layer of the main jet. An increase in the angle between the chevron plane and the jet flow direction intensifies the wake flow.

The flow structure in a supersonic axisymmetric underexpanded jet exhausting from a convergent nozzle with six chevrons at the exit was studied. Interaction of the chevrons with the jet flow leads to transformation of the stationary jet structure and to formation of mushroom-shaped large-scale vortex structures. Numerical simulations of the supersonic underexpanded jet exhausting from the nozzle with chevrons made it possible to determine the structure of the streamwise vortices generated by the vortex-forming element and also to find the specific features of formation of the mushroom-shaped structures in the shear layer. The secondary maximum in the radial distribution of the measured Pitot pressure at the jet boundary is caused by the change in the direction of the initial high-pressure gas flow (first, away from the jet axis, and then toward the jet axis).

ACKNOWLEDGEMENTS

This work is supported by the Russian Foundation for Basic Research (Grant No. 05-08-01215) and by the Siberian Supercomputer Center of the Siberian Branch of the Russian Academy of Sciences.

REFERENCES

[1] Smith A.E., Dussauge J.P. *Turbulent shear layers in supersonic flow*. American Institute of Physics. Woodbury, New York, 1996, 357 p.

[2] Gutmark E.J., Schadow K.S., Yu K.A. Mixing enhancement in supersonic free shear flows, *Annu. Rev. Fluid Mech.* 1995. Vol. 27. pp. 375-417.

[3] Liepman D., Gharib M. The role of streamwise vortices in near-field entrainment of round jets, *J. Fluid Mech.* 1992. Vol. 245. pp. 643-667.

[4] Zapryagaev V.I., Solotchin A.V. *Spatial structure of the flow in the initial section of a supersonic underexpanded jet*. Preprint No. 23-88, Inst. Theor. Appl. Mech., Sib. Branch, Russian Acad. of Sci., Novosibirsk, 1988.

[5] Zapryagaev V.I., Solotchin A.V. Three-dimensional structure of flow in a supersonic underexpanded jet, *J. Appl. Mech. Tech. Phys.* 1991. Vol. 32. No. 4. pp. 503-507.

[6] Zapryagaev V.I., Kiselev N.P., Pavlov A.A. Effect of streamline curvature on intensity of streamwise vortices in the mixing layer of supersonic jets, *J. Appl. Mech. Tech. Phys.* 2004. Vol. 45. No. 3. pp. 335-343.

[7] Krothapalli A., Buzyna G., Lourenco L. Streamwise vortices in an underexpanded axisymmetric jet, *Phys. Fluids. A.* 1991. Vol. 3, No. 8. pp. 1848-1851.

[8] MacCormic D. C., Bennett Jr J. C. Vortical and turbulent structure of a lobed mixer free shear layer, *AIAA J.* 1994. Vol. 32, No. 9. pp. 1852-1859.

[9] Samimy M., Zaman K. B. M. Q., Reeder M. F. Effects of tabs on the flow and noise field of an axisymmetric jet, *AIAA J.* 1993. Vol. 31, No. 4. pp. 609-619.

[10] Khritov K. M., Kozlov V. Ye., Krasheninnikov S. Yu, et al. On the prediction of turbulent jet noise using traditional aeroacoustic methods, *J. Aeroacoustic,* 2005. Vol. 4, No. 3/4. pp. 289-324.

[11] Sayed N., Mikkelsen K., Bridges J. Acoustics and thrust of quiet separate-flow high-bypass-ratio nozzles, *AIAA J.* 2003. Vol. 41, No. 3, pp. 372-378.

[12] Shur M.R., Spalart F. R., Strelets M. Kh. Calculation of noise of complex jets on the basis of the first principles, *Mat. Model.* 2007. Vol. 19, No. 7. pp. 5-26.

[13] Deich M.E. *Technical Gas Dynamics,* Moscow: Energiya, 1974.

[14] Dulov V.G., Luk'yanov G.A. *Gas Dynamics of Exhaustion Processes,* Novosibirsk: Nauka, 1984.

[15] Zapryagaev V.I., Kiselev N.P. Flow structure formed by interaction of a single microjet with a supersonic jet flow, *J. Appl. Mech. Tech. Phys.* 2009. Vol. 50. No. 3. pp. 447-453.

[16] Petunin A.N. *Methods and Techniques of Measuring of Gas Flow Parameters,* Moscow: Mashinostroenie, 1972.